Astron. Astrophys. 342, 279–284 (1999)

ASTRONOMY AND ASTROPHYSICS

Explosive events in the solar atmosphere

M.E. Pérez[1], **J.G. Doyle**[1], **R. Erdélyi**[2,3], **and L.M. Sarro**[4]

[1] Armagh Observatory, College Hill, Armagh BT61 9DG, Ireland (e-mail: epp@star.arm.ac.uk; jgd@star.arm.ac.uk)
[2] Department of Applied Mathematics, University of Sheffield, Hicks Building, Sheffield, S3 7RH, UK (e-mail: Robertus@sheffield.ac.uk)
[3] School of Mathematical and Computational Sciences, University of St. Andrews, North Haugh, St. Andrews. Fife, KY16 9SS, Scotland (e-mail: robertus@dcs.st-and.ac.uk)
[4] Laboratorio de Astrofísica Espacial y Física Fundamental (LAEFF), INTA, P.O. Box 50727, E-28080 Madrid, Spain (e-mail: lsb@laeff.esa.es)

Received 11 August 1998 / Accepted 27 October 1998

Abstract. Two examples of explosive events observed with SUMER in transition region spectral lines are reported here; one detected in C IV 1548 Å, in a region within the northern polar coronal hole, and the other in O VI 1032 Å, in an active region. The event measured in C IV lasted ~ 3 min and extended approximately a region of 8 arc sec along the slit (N-S) and 8 arc sec in the E-W direction. Velocities reached around 150 km s^{-1} in the blue wing and 100 km s^{-1} in the red wing. The active region events were more energetic and in total lasted ~ 6 min. At the point of maximum activity, a region of 8 arc sec along the slit is covered by one explosive event located in the northern section of the observed region, while in the southern section we observe two events very closely located and extended over a maximum of 14 arc sec along the slit. More precisely, in the northern section we have at least two consecutive events occurring in a short time interval ($\sim$ 12 min) separated by $\sim$ 3 arc sec. In the E-W direction the raster length covered by each of these events was approximately 4 arc sec. The explosive events seen in O VI showed a very complex structure of subsonic and supersonic velocity flows, both red-shifted and blue-shifted. The apparent maximum velocity reached in the blue wing was approximately 250 km s^{-1} and 215 km s^{-1} in the red wing.

Key words: Sun: flares – Sun: UV radiation

1. Introduction

With the launch of SOHO new opportunities have become available for studying short-time scale variability phenomena, such as explosive events. The instrument that allows us to do so is SUMER (Solar Ultraviolet Measurements of Emitted Radiation), a stigmatic normal incidence spectrograph operating in the wavelength range 450 to 1610 Å (Wilhelm et al. 1997). In July 1996, we obtained data with SUMER at several locations on the solar disk using two different modes of operation; (i) a sit-and-stare mode and (ii) rastering. Here we report two raster datasets; the first taken in an active region on 10 July 1996 and the second taken on 14 July 1996 in a northern coronal hole region. The observing sequences involved the resonance lines C IV 1548 Å and O VI 1032 Å formed in the transition region between 10^5 and $3\ 10^5$ K.

The phenomena underlying some explosive events has been interpreted as a bi-directional jet. Dere et al. (1991) first suggested such an analysis and recently Innes et al. (1997) have found new evidence to support this interpretation. Innes et al. (1997) found Doppler shifts changing from red to blue within a few arc sec (an offset of 8 arc sec along the slit was observed), and the two wings of the emission moving away from the center of the jet by a distance of 6 arc sec in one case. During the decay of these events the velocities remained large having a lifetime of approximately 4 min. On the other hand, Chae et al. (1998) showed a strong tendency for explosive events to occur repeatedly in bursts. In the present work both previously mentioned characteristics are observed.

The purpose for obtaining this data was to provide input for an ongoing explosive event modelling programme (Erdélyi et al. 1999). The scope of this programme is to study the relevance of the explosive events phenomena in the process of heating the solar corona.

2. Observational data

The first observational dataset reported here was obtained with SUMER on-board SOHO on 10 July 1996 for O VI 1032 Å from an active region SW on the solar disk (see Fig. 1). The observational sequence for this line was designed so that after an integration time of 15 s, the slit was stepped 1.1 arc sec eastward, accumulating a $\sim 66 \times 120$ arc sec^2 image in 15 min (see Table 1). After a preliminary analysis of these data we found a continuous series of raster positions with evidence of explosive events between 630 arc sec and 650 arc sec in the E-W raster direction (see Figs. 7 and 8 later).

The second dataset for C IV 1548 Å was obtained from a region in the northern polar coronal hole (see Fig. 2) on 14 July 1996. For this line the integration time was 20 s and the observational sequence was designed so that after each integration, the slit was again moved 1.1 arc sec eastward, thus rastering a 33×120 arc sec^2 area in 10 min (see Table 1). In the present dataset a continuous series of raster positions was found, after

Send offprint requests to: M.E. Pérez

Table 1. Description of observational data

Date	10 July 1996	14 July 1996
Start UT	07:19:18	06:30:20
Pointing: X,Y	(630,-200)	(2,910)
X Width/Y Width	66×120	33×120
Exposure time	15 s	20 s
Location	AR	Northern CH
Spectral line	O VI 1032	C IV 1548
Log (T_e/K)	5.5	5.0
Solar region	High-Transition Region	Mid-Transition Region

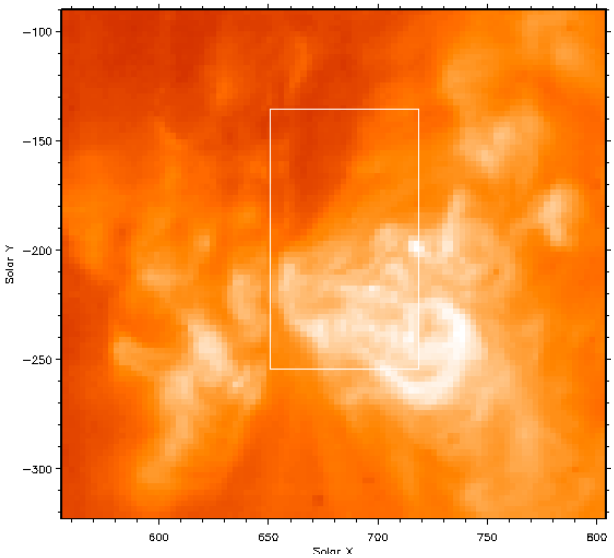

Fig. 1. A SOHO EIT image obtained in Fe XII 195 Å on 10 July 1996 at 20:38 (courtesy of the EIT consortium). The SUMER raster series for O VI were centered −200 arc sec from disk center, i.e., in the active region shown in this zoom image. The SUMER raster dimensions are over-plotted with a white rectangle.

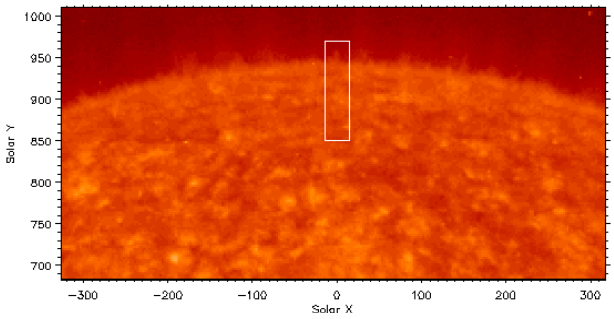

Fig. 2. A SOHO EIT image obtained in He II 304 Å on 14 July 1996 at 18:13 (courtesy of the EIT consortium). The SUMER raster series for C IV were centered 909 arc sec from disk center, i.e., in the northern coronal hole shown in this zoom image. The SUMER raster dimensions are over-plotted with a white rectangle.

analysis, to show evidence of explosive events over a region of $\sim$ 8 arc sec along the slit (N-S direction) and $\sim$ 8 arc sec in the E-W direction (see Figs. 5 and 6 later). Also Si II 1533 Å (formed below $2\ 10^4$ K) was observed in this dataset simultaneously with C IV 1548 Å. These profiles were not affected by any explosive event signature, although its intensity was quite weak in the observed region. As has been shown by previous observations, the incidence of explosive events seems to be limited to transition region lines.

The spatial resolution of SUMER is approximately 1 arc sec in the E-W raster direction and 2 arc sec along the slit, N-S direction. Observations were made in the 1^{st} order of diffraction with the corresponding dispersion of 42–44 mÅ/pixel for the aforementioned wavelengths. The coronal hole observations were taken on the more sensitive central part of detector A, coated with KBr which increases the quantum efficiency by an order of magnitude in the range 900 Å to 1500 Å, while the active region observations were taken on the bare part of the detector. We used the 1×120 arc sec slit for the 14 July dataset and 0.3×120 arc sec slit on 10 July.

2.1. Data reduction and further treatment

For the SUMER instrument, the process of data reduction involves three main steps: flatfielding, destretching and radiometric calibration. Our dataset were automatically flat-field corrected on board SUMER. Destretching of the SUMER dataset is necessary, in particular for the data towards the end of the slit due to various wavelength and spatial distortions in the detector (see Siegmund et al. 1994, Wilhelm et al. 1995). For the above corrections the basic IDL routines can be found from within the SUMER s oftware tree.

In order to improve the fitting of individual spectral profiles it was necessary to apply a filtering process. To preserve our spatial resolution (approximately 2 arc sec N-S and 1 arc sec E-W direction), we analyse individually each position along the slit for each raster position. For the raster positions showing explosive events, the signal-to-noise ratio is good although high frequency noise as still present in the profiles. In order to remove this, an optimal (Wiener) filter was applied to the data (Gray 1992). In Figs. 3 and 4 we show examples of the un-filtered and filtered O VI and C IV profiles for a single pixel during each of the explosive events.

In order to calculate a reference profile, only raster positions free of explosive events were selected, averaging them first along the raster direction (E-W) and afterwards along the slit (N-S). The central wavelength of this reference profile is our rest wavelength, from which we measure velocity shifts. However, the rest wavelength of the observed lines is not constant along the slit. In particular, in the active region dataset the average fluctuations are of the order of ~ 5 km s^{-1} within an area of 5 arc sec and can reach up to ~ 18 km s^{-1} difference between the intense and darker regions along the slit area. To remove this variation, all the raster positions not showing evidence of explosive events (28 for O VI and 20 for C IV) were summed together and a mean wavelength as a function of position along the slit was derived. This difference in wavelength was then applied to

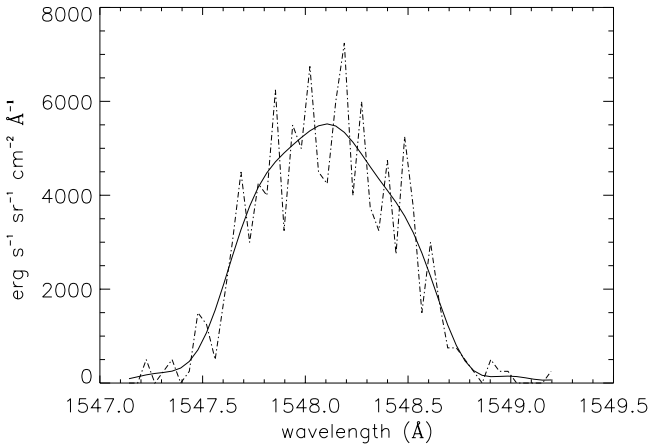

Fig. 3. Optimal filter (solid line) applied to a C IV 1548 Å raw profile (dashed line) located in (X,Y) = (-6,904) arc sec. Frame 06:33:01 UT in Fig. 5.

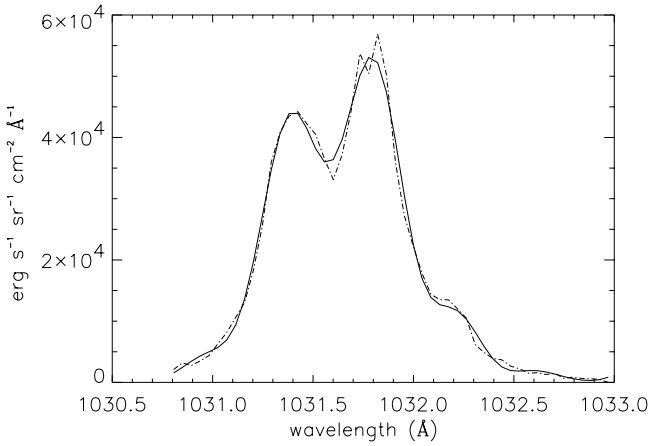

Fig. 4. Optimal filter (solid line) applied to a O VI 1032 Å raw profile (dashed line) located in (X,Y) = (639,-178) arc sec. Frame 07:28:55 UT in Fig. 7.

the individual spectral profiles thus standardising them all to a common wavelength. The above process was then repeated in order to check the accuracy; an uncertainty of 2 km s^{-1} (1σ) was derived.

2.2. Contemporary observations with SOHO

In order to contrast our observations we have checked for contemporary observations done with other instruments on board SOHO, Yohkoh and also ground observations. The most interesting comparison comes out for the data taken on 10 July 1996. From comparison with Yohkoh, EIT and CDS images we can see that our SUMER raster covers an area near the apparent foot points of a complex structure of loops in an active region located SW on the solar disk (see Fig. 1). The structure of this active region remains for more than two days, from 9 July to 11 July 1996.

A Mt. Wilson magnetogram was taken nine hours later than our observations. Our raster coincides with a bipolar magnetic feature in the middle of an active region. At the north of our raster image the emerging magnetic field is weaker than at the south. It is in this northern region where the velocities of the observed explosive events are higher and their incidence prolonged, as will be described in the next section. Other authors have associated explosive events to the cancellation of photospheric magnetic flux and preferentially regions with weak and bipolar magnetic field (Porter et al. 1987, Dere et al. 1991, Moses et al. 1994, Chae et al. 1998).

3. Results

3.1. Coronal hole: C IV 1548 Å

The sequence in Fig. 5 lasts 200 s and covers a solar area of 10×20 arc sec^2. In the first time frame we see a broadening in the C IV line centered at 904 arc sec north of disk center. By the second time frame (06:31:40 UT) we see a blue-shifted component. For the next 40 s, the line is mostly blue-shifted although there is a weak red-shifted feature. At 06:32:41 UT we see another injection of energy resulting in blue and red-shifted plasma, shown more clearly in Fig. 6. By this stage the center of the feature has drifted southward by three to four arc sec. The latter four raster positions show mostly a blue-shifted plasma. The size of the explosive event in the north-south direction had a maximum extent of ~ 6 arc sec. The time frames in Fig. 5 are separated by 1 arc sec (moving eastward), thus the feature is visible over an area of 6×8 arc sec^2. The maximum velocity reached in the blue wing was 150 km s^{-1} and 100 km s^{-1} in the red wing.

An estimation of the characteristic sound speed, c, in a region is given by the relation $c \approx 0.17\, T_e^{0.5}$ km s^{-1}. This implies that for C IV 1548 Å line ($T_e = 10^5$ K) a value for c around 50 km s^{-1} can be estimated. Therefore, we are observing a global presence of supersonic upflows and downflows all along the sequence shown in Fig. 5. We have to consider as well that the Doppler shifts calculated from observations are only a minimum value dependent on line-of-sight conditions for the event.

The line-of-sight conditions for this dataset are particularly extreme being centered as it is in the north pole of the solar disk. This condition makes it especially difficult to observe flows in the radial direction. Further considerations on how that might affect our observations is discussed in the next section.

3.2. Active region: O VI 1032 Å

The first explosive sequence in Fig. 7 lasts for over 4 min. In the first time frame (07:25:37 UT) we see a brightening to the blue at approximately -180 arc sec in the N-S direction, this slowly fades until 07:26:38 UT where we see a broadened blue-shifted line profile with a maximum velocity of approximately 120 km s^{-1}. The mass motion quickly increases in the red wing to velocities of 100 - 150 km s^{-1} by 07:26:53 UT, remaining at these supersonic velocities for 45 s. Similar velocities are seen in the blue wing. The event extends 8 arc sec at maximum and 2 arc sec at minimum in a given raster position. Some apparent displacements along the slit of the highest velocities in

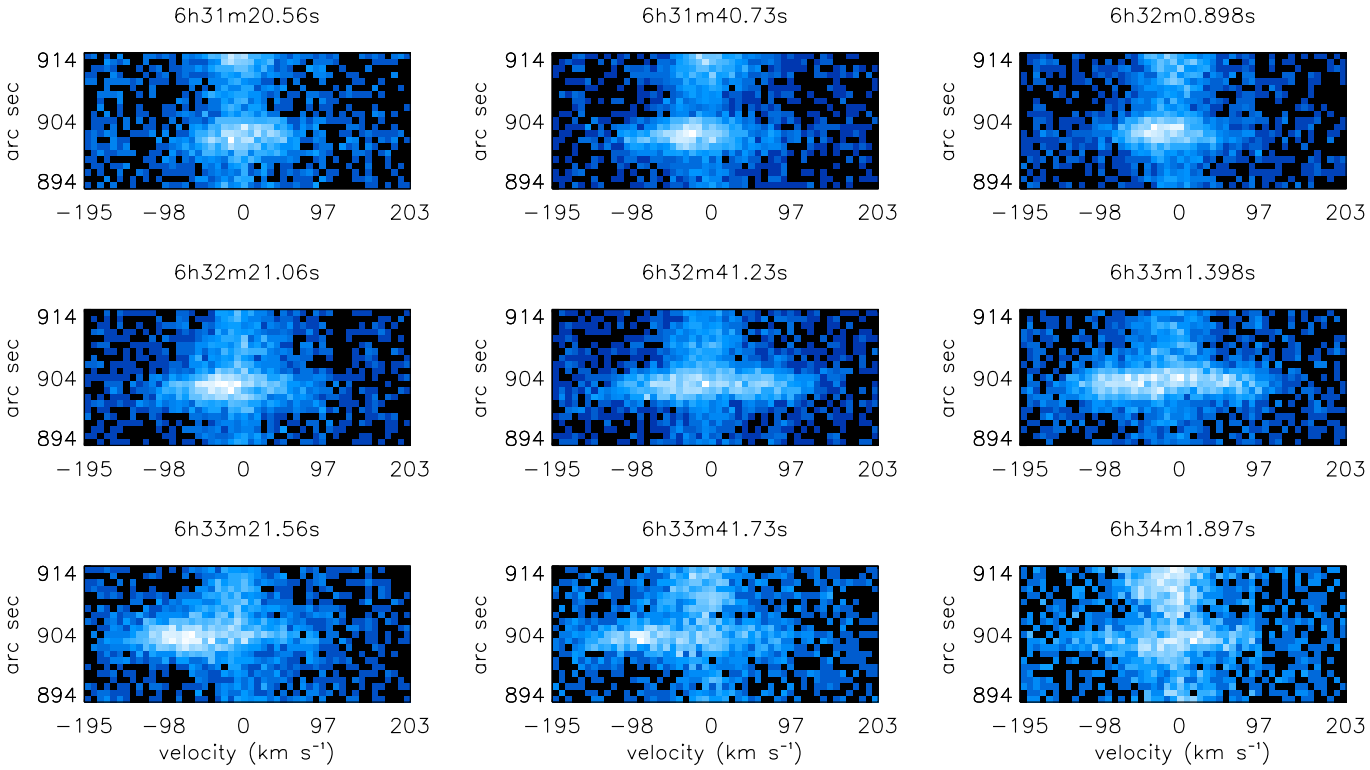

Fig. 5. A time series for an explosive event observed in C IV 1548 Å in a northern coronal hole on 14 July 1996. Doppler velocities are shown in a scale from -195 km s^{-1} (blue-shift) to 203 km s^{-1} (red-shift).

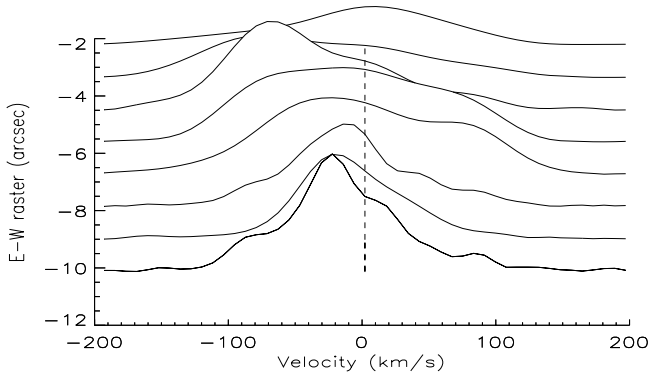

Fig. 6. The C IV 1548 Å line profile averaged over the whole explosive event as a function of time.

the mass flows are observed. In the frames between 07:27:54 UT and 07:28:39 UT the velocities fall below the sound speed ($c \approx$95 km s^{-1}) in the red wing, disappearing at 07:28:39 UT, while they stay very close to the sound speed value for the blue wing over a region of 2 - 4 arc sec along the slit. At 07:28:55 UT there is another injection of energy, with plasma again moving both red-ward and blue-ward at a velocity up to 160 km s^{-1}. By 07:29:40 UT, the major component is blue-shifted at close to 240–260 km s^{-1}. Fifteen seconds later this has almost decayed. The later time frames also showed apparent motions, now southward by 3 - 4 arc sec. This sequence is shown more clearly in Fig. 8a.

At 07:30:26 UT two explosive events takes place simultaneous at approximately -202 and -209 arc sec in the N-S direction, with the maximum velocity being approximately 200 km s^{-1} in the blue and 180 km s^{-1} in the red direction (see Fig. 8b,c). By 07:31:11 UT, both events are gone. These latter events however occur close to a region which showed persistent broadening and evidence for small scale explosive events over an interval of 4 min prior to 07:30:26 UT.

This active region shows a very complex structure which makes it difficult to give an explanation for the supersonic flows found, but it seems probable that what we observe is a burst of explosive events all along the rastered area.

4. Discussion

Chae et al. (1998) showed there is a strong tendency for explosive events to occur repeatedly in bursts. In this case the persistence of supersonic flows along our raster series in the active region (i.e., the O VI data) could be due to bursts of explosive events in the area observed, which are not connected physically with each other. However, the picture is quite complex and not easy to analyse. The fact that the data are simple raster series makes a proper time evolution analysis impossible, but it still allows us to follow the spatial (temporal) expansion of the jet along the rastered region. Our analyses have shown the complex structure of the velocity fields produced by these jets. There are clearly asymmetric profiles with significative fluctuations in intensity. Also the presence of overlapping velocity fields with a

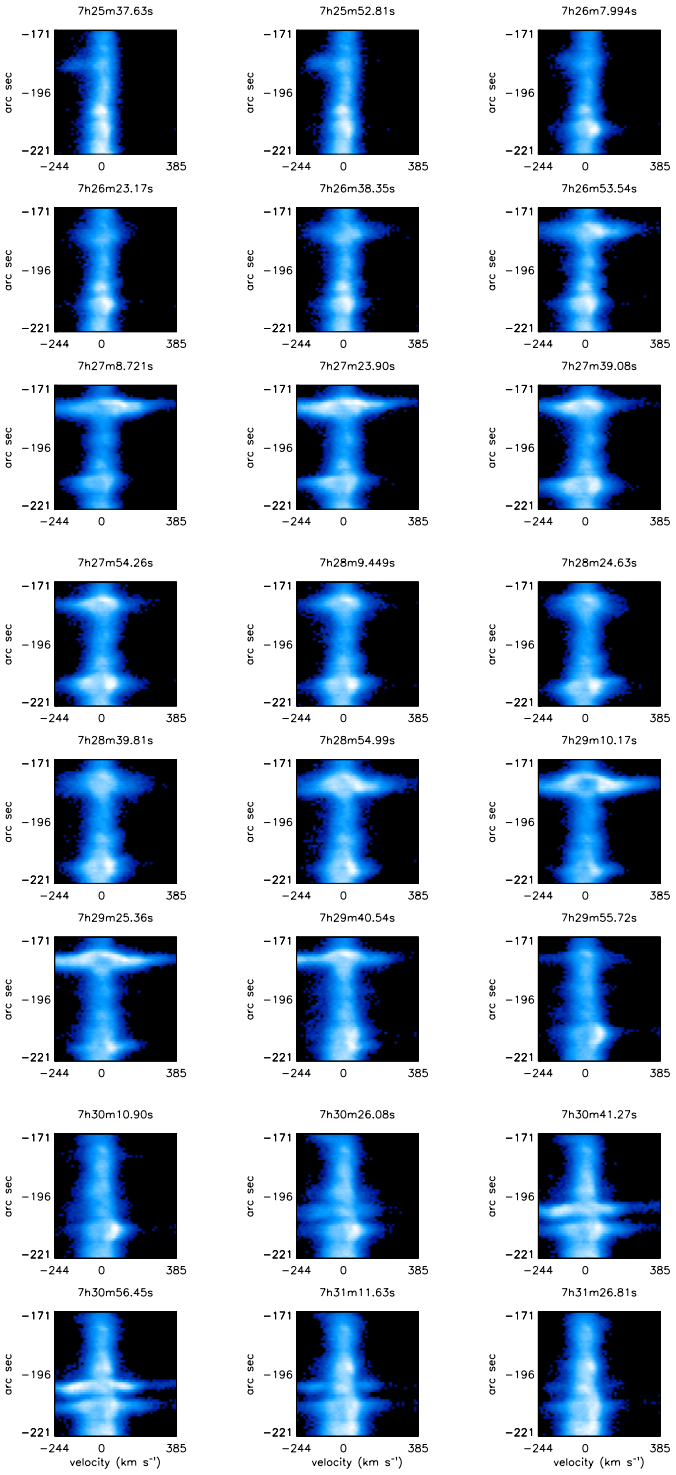

Fig. 7. A time series for an explosive event observed in O VI 1032 Å in a active region on 10 July 1996. Doppler velocities are shown in a scale from $-244\,\mathrm{km\,s^{-1}}$ (blue-shift) to $385\,\mathrm{km\,s^{-1}}$ (red-shift).

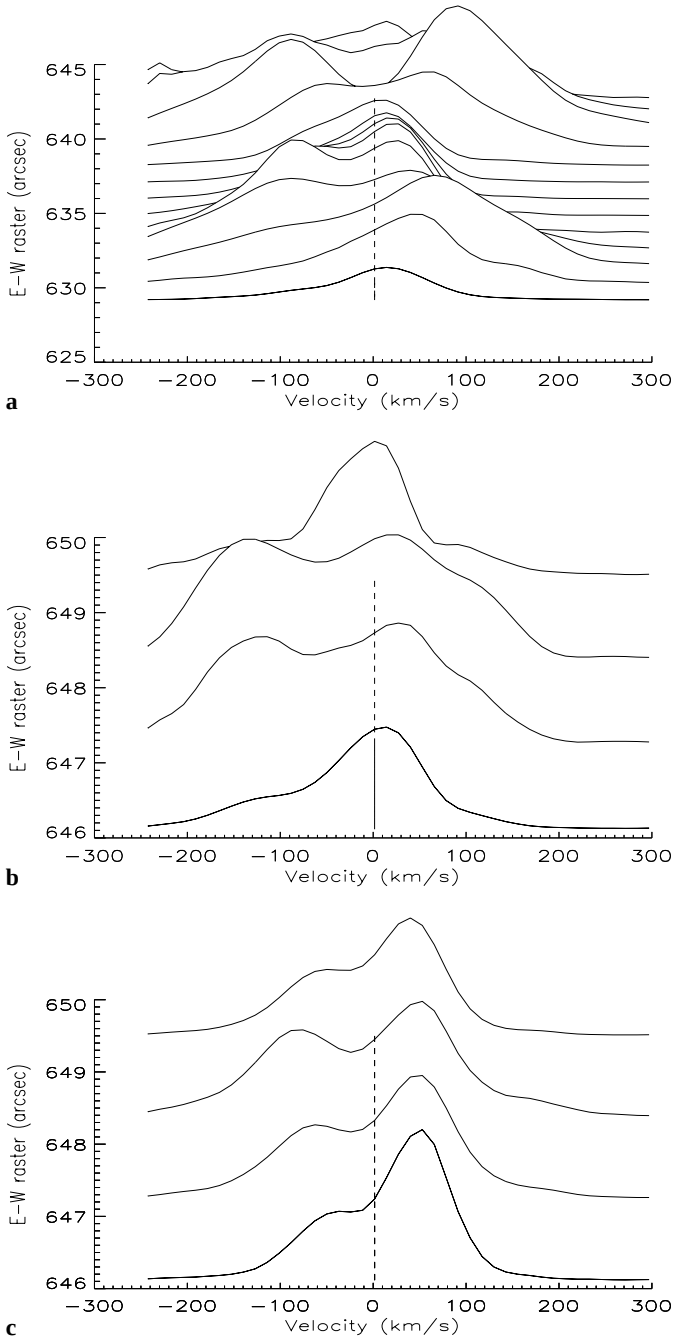

Fig. 8a–c. O VI 1032 Å: For each time frame in the raster series we show here an averaged profile over the whole explosive event with the vertical line showing the zero velocity reference for **a** The first two events in Fig. 7, between 07:28:39 UT and 07:29:40 UT (629–643 arc sec E-W), **b** One of the twin events between 07:30:26 UT and 07:31:11 UT and **c** The other twin event between −210 and −207 arc sec, in the N-S direction.

consistent structure along the slit is apparent, often leading to supersonic flows.

For the C IV data in Figs. 5 and 6, it is not possible to identify the signature as a burst of explosive events given the fact that the supersonic flows are concentrated in a small area along the slit, in a relatively small rastered area. Also, against this idea is the apparent pattern that the flows follow in the E-W direction. The characteristics of this sequence of events can, instead, be compared with those discussed by Innes et al. (1997). If we suppose this sequence is produced by only one jet propagating

away from its source, the area in which it is visible (6×8 arc sec^2) and the observed lifetime ($\sim 160\,s$) would be in coincidence with those previous results of Innes et al. However, the present event does not show clear Doppler shift changes from red to blue along the E-W direction, or any obvious offset of the red and blue-shifts along the slit. Although there are some indications in the last three raster positions of mainly blue-shifted plasma, we still measure weak supersonic flows in the red wing for some positions. For the rest of the frames, in general we find blue-shifted as well as red-shifted profiles for each position along the slit. The maximum velocities, though, correspond to blue-shifts. Globally the blue wing is m ore intense than the red one.

The C IV event can perhaps be explained as a jet of bi-directional nature if we consider a high latitude as a possible explanation for the apparent confusion between the two opposite flows. The jet can be within a plane that forms a short angle with that formed by the line of sight and the E-W direction, and the axis of this jet forms a relatively small angle with the line of sight. This angle could explain the apparent South-to-North motion of the maximum of the blue-shifted velocity fields. That occurs while we raster West-to-East. In these conditions we can explain why the first raster position shows the coincidence of blue-shifts and red-shifts, while the latter ones are mainly blue-shifted. If this is correct, we can assume that the distance that this event covers in our raster (8 arc sec in 160 s) corresponds with its increase of size. If that change in size is due to the propagation of the head of the jet at a velocity equal to its maximum Doppler velocity, approximately 150 km s^{-1}, then we can estimate its length. We calculate an average transverse velocity of 35 km s^{-1} which leads to an inclination angle for the axis of our jet of $\sim 13^\circ$. Then the actual jet length is approximately 35 arc sec or 2.5×10^4 km, estimated from the apparent length of 8 arc sec ($\sim 6 \times 10^3$ km). This extension implies that the jet reaches the corona and travels down along most of the transition region.

An ongoing explosive event modelling programme allows us to convert computational results into UV line profiles in non equilibrium ionization as a function of time (see, e.g., Erdélyi et al. 1997, 1998, Sarro el al. 1997). The early results of the ongoing modelling indicate a sudden deposition of energy below the transition region on one side of the loop resulting in the ejection of cool, dense gas bullets, plus the generation of sound waves. Following, the interactions between the cool gas bullets and sound waves (which develop into shock waves), we have the appearance of 'new' transition regions, moving at different velocities. Although the atomic physics aspect of the simulations are in good shape, the MHD section requires further development and thus detailed comparison with the data is deferred (Erdélyi et al. 1999).

5. Summary

In the northern coronal hole we may have observed a bi-directional jet with an observed velocity range of between 150 km s^{-1} in the blue wing and 150 km s^{-1} in the red wing. The life time for this event is approximately 160 s with a length approximately 35 arc sec. This extension implies that the jet reaches the corona and travels down along most of the transition region. As has been shown by previous observations, the incidence of these explosive events seems to be limited to transition region lines.

In the events observed in the active region the observed velocities range between 250 km s^{-1} in the blue wing to 215 km s^{-1} in the red wing. The life time for these events ranges between 60 to 90 s. As with other authors before us, we have associated the active region explosive events to regions with weak and bipolar magnetic fields. A more detailed comparison of these observations with an ongoing explosive event modelling programme is underway (Erdélyi et al. 1999).

Acknowledgements. Research at Armagh Observatory is grant-aided by the Dept. of Education for N. Ireland while partial support for software and hardware is provided by the STARLINK Project which is funded by the UK PPARC. This work was supported by PPARC grant GR/K43315. We would like to thank the SUMER and EIT teams at Goddard Space Flight Center for their help in obtaining the data. The SUMER project is financially supported by DLR, CNES, NASA, and PRODEX. SUMER is part of SOHO, the Solar and Heliospheric Observatory of ESA and NASA. MEP is supported via a studentship from Armagh Observatory. R.E. would like to thank M. Kéray for patient encouragement. R.E. also thanks the support from PPARC (Particle Physics and Astronomy Research Council) of United Kingdom. This work was also partially supported by the Spanish DGICYT under grant number PB-941275 and the British Council.

References

Chae J., Wang H., Lee C., Goode P.R., Schühle U., 1998, ApJ 497, L109

Dere K.P., Bartoe J.-D.F., Brueckner G.E., 1991, J. Geophysical Res. 96, 9399

Erdélyi R., Doyle J.G., Pérez M.E., 1997, In: The Corona and Solar Wind Near Minimum Activity. ESA SP-404, 353

Erdélyi R., Sarro L.M., Doyle J.G., 1998, In Solar Jets and Coronal Plumes. ESA SP-421, 207

Erdélyi R., Sarro L.M., Doyle J.G., Pérez M.E., 1999, in preparation

Gray D.F., 1992, The Observation and Analysis of Stellar Photospheres. Cambridge University Press

Innes D.E., Inhester B., Axford W.I., Wilhelm K., 1997, Nat 386, 811

Moses D., Cook J.W., Bartoe J.-D.F., et al., 1994, ApJ 430, 913

Porter J.G., Moore R.L., Reichman E.J., Engvold O., Harvey K.L., 1987, ApJ 323, 380

Sarro L.M., de Sterck H., Erdélyi R., Doyle J.G., Montesinos B., 1997, In: The Corona and Solar Wind Near Minimum Activity. ESA SP-404, 657

Siegmund O.H.W., Gummin M.A., Stock J.M., et al., 1994, Proc SPIE 2280, 89

Wilhelm K., Curdt W., Marsch E., et al., 1995, Sol Phy 162, 189

Wilhelm K., Lemaire P.,Curdt W., et al., 1997, Sol Phy 170, 75